Effect of specimen geometry, quenching and trigger mechanism on crushing performance of single hat column

Effect of specimen geometry, quenching and trigger mechanism on crushing performance of single hat column

A R N Izzah [1], Salwani MS[1], Tan SW[1] , Mas Ayu H[1], Rosdi D[1]

[1] Faculty of Mechanical Engineering, Universiti Malaysia Pahang, 26600 Pekan, Pahang, Malaysia

*Corresponding author: salwani@ump.edu.my

Abstract. Paraffin deposition in the crude oil production pipeline has been an alarming problem to the flow assurance community. This phenomenon causes a tremendous amount of material loss in the production and substantial resources are expended to resolve these flow assurance problems—which included the chemical treatment. This study examined an agricultural non-ionic silane-based surfactant and its blends (with silica nanoparticles) as a flow improver using Malaysian light crude oil (42.4°API). In particular, this study performed the following experimental measurements: wax appearance temperature, pour point, viscosity, and FTIR spectroscopic analysis. The result showed that the surfactant-nanoparticles blend affected the viscosity (significant reduction by approximately 67 %) within certain temperature range and were able to depress both pour point (to 4°C) and wax appearance temperature (15.6°C). It was also revealed that the most potent blend consisted 400 ppm of silane-based surfactant and 200 ppm of SiO_2 nanoparticles. The study also evaluated the underlying mechanisms for the variation of viscosity through FTIR spectroscopic analysis.

1. Introduction

Performance of a vehicle can be determined by crash analysis of frontal impact test, overlap test and side impact test. In frontal impact test, the vehicle will impact with a concrete wall at specified speed. In developed countries, frontal crashes have contributed 50–70% of the fatalities during accidents[1]. In other words, more than half of the car accidents involved the front side of the car. Therefore, it is important to study on improvement of the frontal part of the vehicle to increase the passenger's safety during crashes.

For that instance, the crash box was attached between the bumper and side rails in front of the vehicle to absorb initial kinetic energy to ensure a low plastic flow stress level on the vehicle body frame during car crash[2]. The crash box is expected to be collapsed by absorbing crash energy prior to the other body part. Thus, damages of the main passenger's compartment can be minimized to ensure the passengers' safety. During a crash event, it is important to understand the energy of the impact and how the loads are transmitted through the system[3]. Higher energy absorption coupled with lower initial peak force should be achieved to prevent the catastrophic collapse and increased passenger survival chances due to crash or impact[4] Therefore, the axial crushing behaviour of thin-walled structures has been the favourite topic among researchers. Experimental, theoretical and numerical studies on structures under axial loading condition which focused on the crushing behaviour, the peak force and the energy absorption capacity of the structure can be found enormously [3].

Various design of crash box has been studied by researchers to obtain the best crashworthiness characteristic. There are few research papers that compare the crashworthiness of structures with a different cross-section such as circle [5][6], square [7][8] and polygonal [8][9] under different impacting velocities. Other than that, hat-shaped cross section is also often used as an energy absorbing structure. Costas et al. found that energy absorption capacity of all the filled the hat-section specimen increases compared to the empty specimen [1]. An experimental study on a composite structure has shown that energy absorption of a structure improves with the increases of the tube wall thickness [10]. In contrast, energy absorption of aluminium tubes was lower with the increasing of wall thickness due to increases in tube rigidity [11]. The load-displacement curve for stainless steel samples also showed that energy absorption of the thick tube was lower compared to the thin tube [12].

Despite shape configuration, triggering mechanism is perceived as one of the most influential design factors for crashworthy performance. Formation of trigger at appropriate location of the structures caused stress concentration which capable of avoiding the load transfer to the whole structure effectively. It also prevents structures from collapse catastrophically and induces a progressive failure mode to maximize the energy absorption. Moreover, triggering mechanism is an effective method to reduce the maximum crushing load, P_{max} during impact [4].

Although aluminium has high specific strength per weight ratio compared to conventional mild steel, recent research leads to advanced high strength steels (AHSS) with striking characteristics. Material that is on the forefront and highly demanding of innovation in the automotive industry is AHSS (Advanced High-Strength Steel) and UHSS (Ultra High-Strength Steel). AHSS has high-strength and durability but at the same time, formability of the material is maintained. Types of AHSS such as dual phase (DP) steel [13][14] and transformation induced plasticity (TRIP) steels [15] that has higher specific strength. The forming process of UHSS is limited because it has low formability and considerable spring back. In order to solve this, the material is alloyed with boron. Boron is used for enhancing the hardness and strength of alloyed steel [2]. Hence, the size and weight of the steel used can be decreased for the same strength requirement. Mechanical properties and microstructure that required any range of application can be reached by choosing the suitable parameters for heat treatment of the steels. However, the type and parameter of heat treatment can form different microstructures that produce different mechanical properties. This paper studies the effect of heat-treatment on mechanical properties and crushing performance of boron alloyed steel.

Nowadays, many engineering application has been using boron steels as the material. For example, in high strength appliances and wear material. Boron offers hardenability and toughness but lighter structure. By adding boron in steel, it will become more formable and additional strain age suppressed anneals process can be eliminated and lead to the reduction of manufacturing cost. One of the importance of boron steels is that only a little amount of boron can improve the hardenability of materials. But an excessive quantity of boron will make the hardenability and toughness become lower, cause embrittlement and produce hot shortness. Hardenability and toughness of boron also affected by the percentage of carbon that contains in the steel.

The quenched boron steel formed by hot stamping technology as one of the AHSS, possessing an ultimate stress up more than 1500MPa [16] is deemed to be superior in crashing behaviour. The tailored property of the hot stamping steel has become a favourable topic among researchers as the hot stamping technology is developed [17]. The Dual Phase steel's grade can be through water quenching process but still maintain the good ductility. Moreover, the process can increase the ultimate tensile strength up to 1000 MPa. [18] Nishibata and Kojima [19] investigated the effect of the cooling rate on the hardness and toughness of quenched boron steel and achieved the tailored property's mechanism and method. Bardelcik et al. [20] developed the "Tailored Crash Model" (TCM) by using the true stress versus effective plastic strain curves. While Eller et al. [16] has modelled the strain hardening behaviour with a new extended Swift hardening law since the classical hardening law failed to adopt the strain hardening curves of 22MnB5.

Structures undergoing a progressive buckling absorb more energy than structures where a global bending is observed. A way to initiate a reproducible progressive buckling is to introduce imperfections

such as trigger mechanism in the structure[21]. In this study, a trigger mechanism has been introduced at 2 different distances from the impacted side of the structure in order to initiate an anti-symmetrical buckling mode. This paper focuses on the effect of geometry, trigger mechanism and heat quenching rate on the peak force, energy absorption capability and mechanical properties of boron alloyed steel.

2. Experimental section

2.1 Specimen

Specimens are made of boron alloyed steel. In the automotive industry, the Q235A steel is an ideal solution for the construction of structural elements and safety-relevant components in particular in view of the implementation of penetration protection in the areas of the passenger's cabin. Table 1 below shows the chemical composition of boron alloyed steel Q235A that has been used in this research.

Table 1. Chemical composition of Q235A.[22]

Chemical element	Carbon	Silicon	Manganese	Sulphur	Phosphorus	Ferum
wt. %	≤0.22	≤0.35	≤1.40	≤0.050	≤0.045	bal

Two different types of thickness have been prepared for these specimens which are 2 mm and 3 mm. Initially, boron plate was cut into 228mm x 300mm using a shearing machine. Then the plate bent into the hat shape as in figure 1(a) using a bending machine. Many constraints spot-weld were set between the flange of the hat section and a plate closing behind to make the bond of two structure. Then trigger was formed on the hat shape according to the design as in figure 1(b). The distance for each design was measured and the trigger was formed using a grinder.

First, all the specimen was heated in the furnace up to 950℃ for 2 hours. Then, the initial temperature of the specimen was measured by using the infrared thermometer (range -50℃ to 1150℃) right after it was taken out of the furnace. Later, six specimens from two different triggering distances were soaked into the cooled water at 10℃, three of them were cooled for 3 seconds while another three specimens for 8 seconds and the final temperature of the specimen was taken. Then, last six specimens from different triggering distance were taken out and cooled in water at 15℃, three of them were cooled for 3 seconds while another three specimens for 8 seconds and the final temperature of the specimen was taken. The temperature was taken to calculate the cooling rate for each type of quenching process in both types of water. Notation for the specimens are as follows: Thickness-temperature of water-quenching time; No heat treatment (NH) and No trigger (NT). Illustration of the hat section can be referred in Figure 1.

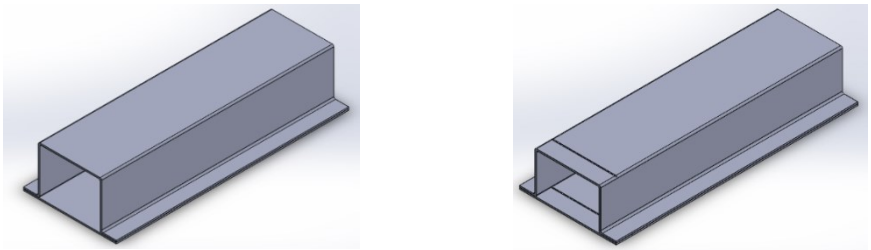

(a) **(b)**

Figure 1. Single hat column (a) without trigger (b) with trigger

2.2 Experimental procedures

Tensile test was conducted using Instron universal testing machine (UTM) based on the ASTM E8 to determine the material properties of each specimen. Since the material is in form of sheet, which is used for hot stamping, it is important to study the behaviour of the rolled sheet using tensile test. For the tensile testing, boron steel plate was cut into dimension as specified in ASTM 08M. All of the specimens were tested subjected to velocity of the top platen plate which set at 1mm/min.

While, the axial compressive testing of the specimens was performed by applying uniaxial quasi-static compressive forces using a Shimadzu SES 1000 universal test machine with loading capacity of 1000 kN. The crosshead speed used was 5 mm/min. Crashworthiness parameters considered include peak force and absorbed energy

3. Results and discussion

3.1 Quenching rate data

Data of temperature of the specimen after taken out from the furnace (T_b) and after being cooled in the water after a certain time (T_a) were measured and recorded in Table 2. The quenching rate for each configuration were calculated using this formula and recorded.

$$Quenching\ rate = \frac{(Temperature\ after\ taken\ out\ from\ furnace - Temperature\ after\ cooled\ in\ the\ water)}{Quenching\ time}$$

Table 2. Quenching rate of the single hat specimens

Thickness (mm)	2			3		
*Specimen	T_b(°C)	T_a(°C)	Quenching rate (°C/s)	T_b(°C)	T_a(°C)	Quenching rate (°C/s)
10-3	775.0	67.3	235.9	789.0	114.0	225.0
10-8	788.0	57.8	91.3	780.1	53.3	90.9
15-3	776.0	68.0	236.0	763.5	172.3	197.1
15-8	773.4	48.3	90.6	762.0	51.3	88.8

***Note: The specimen is labelled according to temperature of water - quenching time**

Data of temperature shown that temperature drop of the thicker specimen is faster than the thinner specimen. This result was supported by Noh study that found out the temperature experienced a time delay with the increasing of tube thickness [27]. Quenching rate of the specimen with lower quenching time obtain are higher compared to the specimen with higher quenching time. Calculated data shown that the quenching rate of the thicker specimen is slower compared to the thinner specimen.

3.2. Tensile test result

Ultimate tensile strength, yield stress and Young's modulus can be observed directly from the stress-strain curve produce from the tensile test. The test was conducted referring to Standard Test Methods for Tension Testing of Metallic Materials (ASTM E8/E8M). The graph for all results was summarized in Figure 3 and 4. Based on Table 3, stress at break of the specimen with heat treatment is higher compared to the original specimen (2-NH). This is caused by the quenching process that toughens and harden the material. After quenching, the material should possess a tempering process to release the

stress and improve toughness. [23] Tempering is important to achieve the ductility without releasing too much hardness. Without the tempering process, the material will lose its ductility and becomes more brittle.

Table 3. Material properties of 2 mm thickness boron alloyed steel

*Specimen	Quenching rate (°C/s)	Young Modulus [MPa]	Stress at Break [MPa]
2-NH	NIL	2,966.55	347.421
2-10-3	235.9	9,733.40	617.005
2-10-8	91.3	8,570.49	387.823
2-15-3	236.0	15,766.67	415.562
2-15-8	90.6	11,884.21	484.041

***Note: The specimen is labelled according to thickness - temperature of water - quenching time, NH: No Heat treatment**

Hardness and toughness of materials highly dependent on the grain size. While the grain size is affected by the quenching rates of the specimen. Therefore, the higher quenching rates will produce harder and stronger materials [24]. Moreover, low quenching rate makes sufficient time for the atoms to achieve the equilibrium condition and have lower quantity of free volume. Low amount of free volume will lead to increases in hardness and toughness of the material. [25]

It can be observed that Young's Modulus of the original specimen (2-NH) is low compared to other specimens that have been quenched. By comparing the specimens with heat treatment, the value of Young's Modulus of 2-10-3 (higher quenching rate) was higher than specimen 3-10-8 (lower quenching rate). Similar results obtained by specimen 2-15-3 (higher quenching rate) which has higher Young's Modulus than specimen that has slower quenching rate (2-15-8). Data from tensile test for the specimen with 3 mm thickness were shown in Table 4.

Table 4. Material properties of 3 mm thickness boron alloyed steel

Specimen label	Quenching rate (°C/s)	Young Modulus [MPa]	Stress at Break [MPa]
3-NH	NIL	3,570.48	383.950
3-10-3	225.0	9,733.40	678.323
3-10-8	90.9	8,470.73	654.740
3-15-3	197.1	10,784.44	441.807
3-15-8	88.8	7,046.02	665.164

Generally, it can be observed from Table 4 that Young's Modulus of the original specimen (3-NH) is low compared to other 4 specimens that have been quenched. Young's Modulus of 3-10-3 (higher quenching rate) was higher than specimen 3-10-8. Quite same results gained by specimen 3-15-3, Young's Modulus is higher than specimen that has slower quenching rate (3-15-8). Results of tensile test for the specimen with 2mm thickness were plotted in a stress-strain curve in Figure 2.

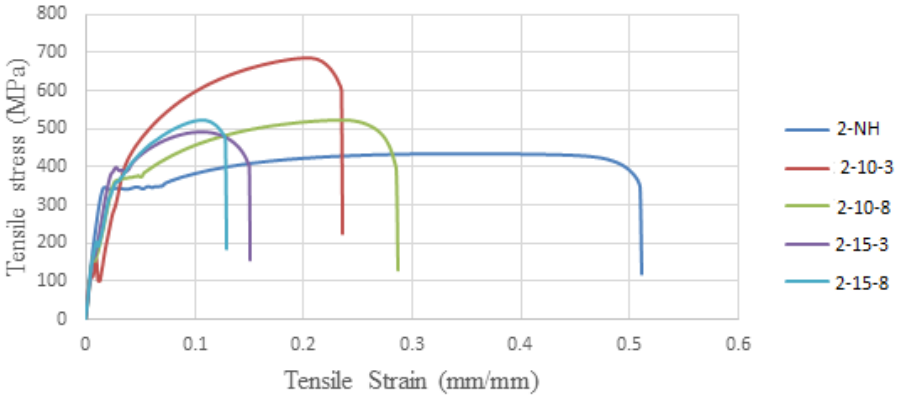

Figure 2. Stress-strain curve of specimen with 2 mm thickness

From Figure 2, it is shown that ductility of the original specimen (2-NH) is higher than the specimen with heat-treatment. While the tensile stress of the specimens with heat-treatment is higher than the original specimen (2-NH). This data proved that the quenching process increases the strength but decrease the ductility of the material. Results of tensile test for the specimen with 3mm thickness were plotted in a stress-strain curve in Figure 3.

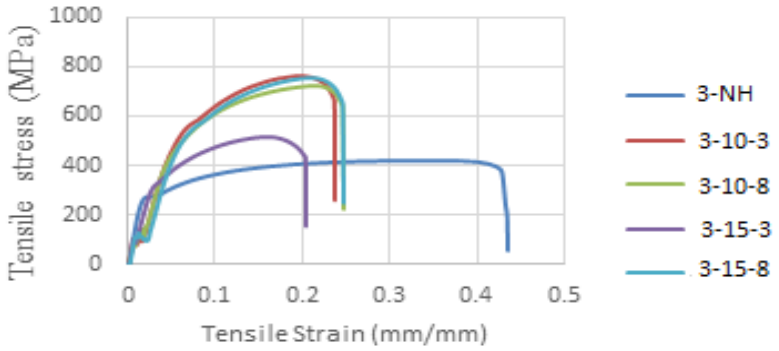

Figure 3. Stress-strain curves for specimen with 3mm thickness

Observation on Figure 3 shown that ductility of the original specimen (3-NH) is higher compared to all the specimens with heat-treatment. While the tensile stress of the specimens with heat-treatment is higher compared to the original specimen (3-NH). This data proved that the quenching process increases the toughness but decrease the ductility of the material.

3.3. Compression test

In compression test, data of peak force and energy absorption capacity can be obtained. This test was conducted using the Shimadzu SES 1000 universal testing machine at 5mm/min. The experiment will stop when the specimen welding was broken. Data obtained from the experiment was recorded in Table 5. Energy absorption for each specimen was calculated from the area under the curve from a force-displacement graph.

Table 5. Experimental data of the compression test for the hat shape boron alloyed

Thickness (mm)	Distance of trigger (mm)	Quenching Water temperature (°C)	Quenching time (s)	Peak Force (kN)	Energy absorption (J)
2	No trigger	Normal water	-	178.06	739.3
	20	Normal water	-	160.63	873.4
	20	10	3	177.94	1017.7
	20	10	8	190.06	745.0
	20	15	3	186.03	681.3
	20	15	8	185.25	1030.5
	40	Normal water	-	135.28	698.4
	40	10	3	199.59	616.5
	40	10	8	188.06	933.9
	40	15	3	204.41	306.4
	40	15	8	199.09	934.1
3	No trigger	Normal water	-	229.50	541.9
	20	Normal water	-	277.50	1037.8
	20	10	3	395.63	1257.4
	20	10	8	376.84	1245.5
	20	15	3	358.38	1230.4
	20	15	8	346.44	1216.7
	40	Normal water	-	272.34	540.5
	40	10	3	381.88	630.4
	40	10	8	380.38	917.6
	40	15	3	264.81	357.1
	40	15	8	328.28	460.0

3.3.1 Effect of thickness .Table 5 shows that for a column with no trigger and quenched in normal water, the energy absorption decreases with the increasing of thickness. Similar results were found by Khalili et al [11] and Kalhor[12] in his study. As for column that trigger employs at 20mm distance, the energy absorption values are increasing with the increasing of thickness. This results aligned with Marzbanrad study on a different geometry of steel [26]. While for columns which trigger employs at 40mm, the energy absorption increase for the column with higher quenching rate but for the column with slower quenching rate, the energy absorption is decreased.

In terms of peak force, it increases with the increase of the column's thickness for all configuration. This is caused by force needed to compress the 3mm column were higher than the 2mm column because the thicker material was more rigid.

3.3.2 Effect of triggering distance. Peak force of the column with a trigger mechanism is higher than the non-triggered columns. Presence of trigger usually reduce the peak force of the column but the location of the trigger must be appropriate to make it efficient. It has been proven in a study conducted by Khalili et al[11]. Only column 2-10-8, 3-10-3, 3-15-3 and 3-15-8 tends to reduce the peak force with the increasing of triggering distance. Basically trigger is introduced to initiate progressive folding [11] that leads to increase energy absorption. This was consistent with the result of specimen 2-10-8. Hence, the energy absorption for almost all the column were decreasing with the increases of triggering distance. This is caused by the poor welding quality that makes the welding to fail during compression. On the other hand, the column tends to bend at the trigger location. Bending part will lower the energy absorption of the column.

3.3.3. Effect of quenching water temperature. From the table, results shown that most of the peak force was decreases with the increases of quenching water temperature for all the 3mm thickness specimen and specimen with 20 mm triggering distance with 8s quenching time for 2mm thickness column,

Moreover, for energy absorption values, most of it was decreased with the increases of quenching water temperature except for 20 mm triggering distance with 8s quenching time and 40 mm triggering distance with 8s quenching time for 2mm thickness column.

3.3.4. Effect of quenching time. As for the different values of quenching time, most of the peak force decreased with the increasing of quenching time for both quenching water temperature except for 20 mm triggering distance with10℃ quenching temperature for 2 mm thickness column and 40 mm triggering distance with 15℃ quenching temperature for 3 mm thickness column.

While for energy absorption, the energy absorption values were increases with the increases of quenching time except for 20 mm triggering distance with10℃ quenching temperature for both thickness and 20 mm triggering distance with15℃ quenching temperature for 3mm thickness specimen.

4. Conclusion

In conclusion, the heat treatment performed on boron alloyed steel with a different type of triggering distance, specimen geometry and quenching condition has portrayed different values on crushing performance of the hat shape column. The use of triggering mechanism was found to be effective only if it employs at the appropriate location. Instead of that, increase in column thickness also increase the energy absorption value and peak force. Values of Young's Modulus and stress at break were higher for the specimen with heat treatment compared to the original one. Column with lower quenching rate possesses higher strength compared to the column with higher quenching rate. Specimen 2-10-3 and 2-15-8 with triggering distance of 20 mm has identified as optimum design as they have high energy absorption capacity with slightly low initial peak force.

Acknowledgment

The author would like to acknowledge the support of the internal grant of Universiti Malaysia Pahang, RDU1803116 and support provided by the Ministry of Higher Education, Malaysia under Fundamental Research Grant Scheme, RDU160140.

References

[1] M. Costas, J. Díaz, L. E. Romera, S. Hernández, and A. Tielas, "Static and dynamic axial crushing analysis of car frontal impact hybrid absorbers," *Int. J. Impact Eng.*, vol. 62, pp. 166–181, 2013.

[2] H. C. Kim, D. K. Shin, J. J. Lee, and J. B. Kwon, "Crashworthiness of aluminum/CFRP square hollow section beam under axial impact loading for crash box application," *Compos. Struct.*, vol. 112, no.

1, pp. 1–10, 2014.
[3] C. P. Gameiro and J. Cirne, “Dynamic axial crushing of short to long circular aluminium tubes with agglomerate cork filler,” *Int. J. Mech. Sci.*, vol. 49, no. 9, pp. 1029–1037, 2007.
[4] H. Jiang, Y. Ren, B. Gao, J. Xiang, and F. G. Yuan, “Design of novel plug-type triggers for composite square tubes: enhancement of energy-absorption capacity and inducing failure mechanisms,” *Int. J. Mech. Sci.*, vol. 131–132, no. June, pp. 113–136, 2017.
[5] A. K. Toksoy and M. Güden, “The strengthening effect of polystyrene foam filling in aluminum thin-walled cylindrical tubes,” *Thin-Walled Struct.*, vol. 43, no. 2, pp. 333–350, 2005.
[6] N. Movahedi and E. Linul, “Quasi-static compressive behavior of the ex-situ aluminum-alloy foam-filled tubes under elevated temperature conditions,” *Mater. Lett.*, vol. 206, pp. 182–184, 2017.
[7] G. Sun, T. Pang, C. Xu, G. Zheng, and J. Song, “Energy absorption mechanics for variable thickness thin-walled structures,” *Thin-Walled Struct.*, vol. 118, no. April, pp. 214–228, 2017.
[8] G. Zheng, S. Wu, G. Sun, G. Li, and Q. Li, “Crushing analysis of foam- fi lled single and bitubal polygonal thin-walled tubes,” *Int. J. Mech. Sci.*, vol. 87, pp. 226–240, 2014.
[9] P. Zhou, E. Beeh, M. Kriescher, H. E. Friedrich, and G. Kopp, “Experimental comparison of energy absorption characteristics of polyurethane foam-filled magnesium and steel beams in bending,” *Int. J. Impact Eng.*, vol. 93, pp. 76–87, 2016.
[10] S.K Subramaniyan, S. Mahzan, M.I. Ghazali, A.M. Zaidi, P.K. Prabagaran. "Energy Absorption Characteristics of Polyurethane Composite Foam-Filled Tubes Subjected to Quasi-Static Axial Loading". *In Applied Mechanics and Materials*.Trans Tech Publications Vol. 315, pp. 872-878, 2013.
[11] A. M. S. H. and K. A. – K. P. Khalili, F. Tarlochan, “Energy absorption capability of thin-walled aluminium tubes under crash loading,” *J. Mech. Eng. Sci.*, vol. 9, no. December2015, pp. 1734–1743, 2015.
[12] R. Kalhor and S. W. Case, “The effect of FRP thickness on energy absorption of metal-FRP square tubes subjected to axial compressive loading,” *Compos. Struct.*, vol. 130, pp. 44–50, 2015.
[13] G. Moeini, A. Ramazani, V. Sundararaghavan, and C. Koenke, “Micromechanical modeling of fatigue behavior of DP steels,” *Mater. Sci. Eng. A*, vol. 689, no. February, pp. 89–95, 2017.
[14] N. Saeidi, F. Ashra, B. Niroumand, and F. Barlat, “EBSD study of micromechanisms involved in high deformation ability of DP steels,” vol. 87, pp. 130–137, 2015.
[15] V. S. Y. Injeti, Z. C. Li, B. Yu, R. D. K. Misra, Z. H. Cai, and H. Ding, “Macro to nanoscale deformation of transformation-induced plasticity steels : Impact of aluminum on the microstructure and deformation behavior,” vol. 34, pp. 745–755, 2018.
[16] T. K. Eller, L. Greve, M. T. Andres, M. Medricky, A. Hatscher, V. T. Meinders, and A. H. Van Den Boogaard, “Plasticity and fracture modeling of quench-hardenable boron steel with tailored properties,” *J. Mater. Process. Technol.*, vol. 214, no. 6, pp. 1211–1227, 2014.
[17] M. Merklein, M. Johannes, M. Lechner, and A. Kuppert, “A review on tailored blanks - Production, applications and evaluation,” *J. Mater. Process. Technol.*, vol. 214, no. 2, pp. 151–164, 2014.
[18] Q. Meng, J. Li, J. Wang, Z. Zhang, and L. Zhang, “Effect of water quenching process on microstructure and tensile properties of low alloy cold rolled dual-phase steel,” *Mater. Des.*, vol. 30, no. 7, pp. 2379–2385, 2009.
[19] T. Nishibata and N. Kojima, “Effect of quenching rate on hardness and microstructure of hot-stamped steel,” *J. Alloys Compd.*, vol. 577, no. SUPPL. 1, pp. S549–S554, 2013.
[20] A. Bardelcik, M. J. Worswick, S. Winkler, and M. A. Wells, “A strain rate sensitive constitutive model for quenched boron steel with tailored properties,” *Int. J. Impact Eng.*, vol. 50, pp. 49–62, 2012.
[21] L. Durrenberger, X. Lemoine, and A. Molinari, “Effects of pre-strain and bake-hardening on the crash properties of a top-hat section,” *J. Mater. Process. Tech.*, vol. 211, no. 12, pp. 1937–1947, 2011.
[22] C. Zeng, W. Tian, W. Liao, and L. Hua, “Study of laser cladding thermal damage : A quanti fi ed microhardness method,” *Surf. Coat. Technol.*, vol. 236, pp. 309–314, 2013.
[23] M. Wang and Z. Liu, “Effects of Ultra-Fast Cooling After Hot Rolling and Intercritical Treatment on Microstructure and Cryogenic Toughness of 3.5%Ni Steel,” *J. Mater. Eng. Perform.*, vol. Voume

26, no. Issue 7, pp. 3016–3024, 2017.

[24] M. Raffik and S. M. Salleh, "Effect of heat-treatment on the hardness and mechanical of Boron Alloyed Steel," vol. 1014, 2017.

[25] D. Singh, D. Singh, R. K. Mandal, O. N. Srivastava, and R. S. Tiwari, "Effect of quenching rate on the microstructure and mechanical behavior of Ce 75 Al 21 Ga 4 glassy alloy," *Mater. Charact.*, vol. 134, no. September, pp. 18–24, 2017.

[26] J. Marzbanrad, "An energy absorption comparison of square , circular , and elliptic steel and aluminum tubes under impact loading An energy absorption comparison of square , circular , and elliptic steel and aluminum tubes under impact loading," no. December, 2016.

[27] Jung-Hun Noh, Dong-Bin Kwak & Se-Jin Yook (2018) Effects of wall thickness and material property on inverse heat conduction analysis of a hollow cylindrical tube, Inverse Problems in Science and Engineering, 26:9, 1305-1325, DOI: 10.1080/17415977.2017.1400027